Technical Assessment of On-Load Tap-Changers in Flemish LV Distribution Grids

Nikolaos Efkarpidis*, Carlos Gonzalez*, Thomas Wijnhoven*,
Daniel Van Dommelen*, Tom De Rybel* and Johan Driesen*
* ESAT/ELECTA, KU Leuven,
Heverlee, Belgium
Email: Nikolaos.Efkarpidis@esat.kuleuven.be

***Abstract*—The increasing electric power consumption and the high penetration level of distributed energy resources (DER) are expected to result in higher loading of Flemish LV distribution grids. A move towards active network management strategies will guarantee the coordinated DER utilization, allowing considerable enhancement of the total connectable distributed generation (DG) and load capacity. The paper describes technical benefits of distribution transformers with on-load tap-changer (OLTC) implemented in a Flemish LV distribution grid. From the assessment, it was concluded that the OLTC partly eliminates the violations of both voltage statutory limits and thermal constraints, however, voltage unbalances can increase due to the independent tap-changing control per phase.**

***Index Terms*—on-load tap-changer, thermal constraints, power quality, voltage unbalance.**

I. Introduction

Recently, two trends have led to higher loading of LV distribution networks. These include increased electric power consumption and distributed energy resources (DER) integration. Although modern devices, such as refrigerators, lighting and washing machines are increasingly efficient consuming less energy, the number of IT and other domestic electric appliances is growing. The increased power requirements demand higher currents causing higher voltage drops along the series impedance of both transformer and lines.

On the other hand, a number of combined influences such as the liberalization of energy markets and growing environmental concerns result in high DER diffusion in LV distribution grids. However, the envisaged, widespread penetration of distributed generation (DG) in distribution networks is expected to result in a variety of well-documented technical impacts relating to power quality, potential equipment overloads and distribution system efficiency [1], [2]. As for the power quality, voltage rise effects have been reported as the foremost concern against the increased DG integration [3], [4]. At present, voltage regulation in Flemish LV distribution networks is not performed automatically, but through the use of manual, off-load tap changers. Typically, the tap positions are calibrated and changed only in case of network extension or modification. Furthermore, the installation of additional, parallel running cables or the replacement of the existing cables by new cables with higher cross section is electro-technically considered a straightforward solution [5]. In spite of further advantages, such as maintenance absence, long durability and protective devices simplicity, high investment costs demotivate their application. Apart from high underground engineering costs, the public acceptance of construction sites on streets and sidewalks is not particularly high. A further alternative is the reduction of cable lengths. However, the main drawback of this method is the high number of substations, leading to higher costs and increased complexity. The meshed multi-directional power flows caused by the progressive DG integration and electric power consumption will induce numerous barriers in daily voltage trend forecasts so that the validity of the traditional local control practices will become inherently inadequate.

Notwithstanding this, a required move towards active network management (ANM) strategies and technologies is expected to significantly enhance the total connectable DG and load capacity. Even though the majority of ANM research has been done at the MV level, several emerging technologies have been investigated for the LV level without massive actual implementation [6], [7]. One of these methods is the application of OLTC at MV/LV distribution transformers. Although OLTC can offer various benefits, it has not yet been incorporated in LV networks by reason of its cost, perceived complexity and state of development.

The main purpose of this paper is to analyze the technical aspects of OLTC, assessing the degree to which its implementation can improve the grid power quality and efficiency in the most effective manner. The proposed OLTC voltage control strategy is analyzed in section II. Several technical impacts caused by anticipated high penetrations of DER and modern electric appliances is the topic tackled in section III. The thermal models of the distribution transformer and the underground cables are considered as well. Finally, the simulation assumptions and the assessment results are presented in section IV.

II. Distribution Transformer with OLTC

Until recently, the application of OLTC was conventially limited to HV/HV or HV/MV transformers, while the small, low-cost distribution transformers did not warrant the expense and complexity of OLTC and were thus normally provided with off-circuit taps. This arrangement enabled the tap positions to be adjusted to suit the network conditions, usually when the transformer was initially placed into service. However, the facility enabled adjustments to be made subsequently, when possible changes to the network loading have necessitated this. [8].

The traditional OLTC control system measures the voltage and load current, estimates the voltage at a remote point and triggers the tap-changer when the estimated voltage is out of

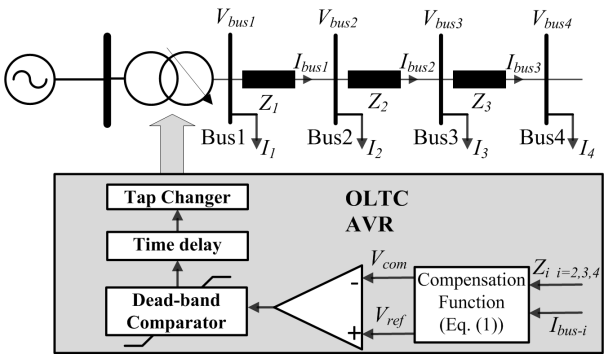

Fig. 1. Traditional line drop compensation control of AVR

bounds. Fig. 1 shows the traditional line drop compensation (LDC) control strategy of the active voltage regulator (AVR). This method feeds back the voltage at the secondary side of the transformer, using the secondary side transformer current, to estimate the voltage drop between the transformer and the load at the end of the feeder [9]. The compensation function V_{com} for the voltage control of bus 4 is shown in (1).

$$V_{com} = V_{bus1} - Z_1 I_2 - (Z_1 + Z_2) I_3 - (Z_1 + Z_2 + Z_3) I_4 \quad (1)$$

V_{bus1} can be locally measured on the transformer secondary side, while the load bus currents I_2,I_3,I_4 and the line impedances Z_1,Z_2,Z_3 can be estimated. However, high DG penetration and gradual load modification will increase the difficulty of current prediction leading to possible failures of the above described method. In accordance to the voltage control method, different control strategies have been reported in the literature for the AVR [10]–[12]. Though the conventional voltage control represents the most straightforward method maintaining the transformer low voltage at a certain level, possible power quality violations of the nodes at the end of a feeder reduce its reliability [10]. Using conventional OLTC control could save investment and operational costs for additional information and communication technologies (ICT), but may have other technical drawbacks like unintended tap settings due to misinterpretations of non-measured values.

Instead of maintaining the substation secondary voltage in a preset tolerance band, the applied control strategy utilizes remote voltage measurement values from all the points of common coupling (PCC's). The proposed OLTC control algorithm of AVR is applied to each phase individually. One unit calculates the minimum U_{min} and the maximum U_{max} value of the n PCCs voltage magnitudes U_1,U_2,...,U_n over a period of time. A tap changer event is triggered, if one of the following conditions becomes true:

$$\Delta tap = \begin{cases} +1, & \text{if } (U_{min} < U_L) \cup (U_{max} < U_H) \\ -1, & \text{if } (U_{min} > U_L) \cup (U_{max} > U_H) \\ -1, & \text{if } (U_{min} < U_L) \cup (U_{max} > U_H) \\ & \quad \cup (\Delta U_{max} - \Delta U_{min} > U_{step}) \\ +1, & \text{if } (U_{min} < U_L) \cup (U_{max} > U_H) \\ & \quad \cup (\Delta U_{min} - \Delta U_{max} > U_{step}) \end{cases} \quad (2)$$

where:

ΔU_{max}	$= U_{max} - U_H$
ΔU_{min}	$= U_L - U_{min}$
U_L	minimum allowable voltage
U_H	maximum allowable voltage
U_{step}	step voltage per tap-change
tap	position of the tap-changer

The range of the transformer ratio in percent above and below, respectively, and the number of the steps depend on the design of the transformer and the OLTC. The voltage between the taps is the step voltage, and it normally lies between 0.8% and 2.5% of the rated voltage of the transformer [13]. In addition, the width of the steps cannot be arbitrarily large as the change of the tap would be too noticeable to the customers.

When the minimum and maximum grid voltage exceed the statutory limits simultaneously, both voltage deviations cannot always be alleviated. The tap-changer event is not triggered when the difference between the marginal voltage deviations is lower than the step voltage. Otherwise, any possible tap-change might mitigate the higher voltage deviations aggravating the lower ones.

Finally, a time setting delay of 5 sec is used for the tap-changing time. This time interval depends on the OLTC architecture and normally is the shortest in solid-state and longest in mechanical OLTC's [14]. In this work, the selection of this value has been made considering a mechanical architecture. The AVR retrieves the voltage measurement data from the remote units every 2 s according to the integration time constant of the simulation. The tap-changer range, the additional voltage step per tap and the number of tap-change steps are determined by the minimum and maximum voltages of the one year load flow calculations.

III. Technical Impacts on LV Distribution Grids

Various technical constraints that determine the response of Flemish LV networks are reported in [15]. In this section, the following three are described: (i) customer voltage rise/drop; (ii) voltage unbalance; and (iii) cable and transformer thermal limits. Regarding the thermal constraints, the thermal models of an oil-immersed distribution transformer and an underground distribution cable are analyzed.

A. Customer voltage rise/drop

In Belgium, DSO's have the obligation to supply their customers at a steady-state voltage within the specified limits of 230 V +10%/-10% for LV distribution networks. According to the standard EN-50160 [16], "Voltage characteristics of electricity supplied by public electricity networks," the 10 minutes mean r.m.s voltage shall not exceed the statutory limits (253 V; 207 V), during 95% of the week. In addition, all 10 minutes mean r.m.s voltages shall be within the range of the 230+10% and 230-15% (253 V; 195,5 V).

As for unbalanced four-wire LV distribution networks, the voltage rise due to return flowing in the neutral conductor needs to be considered in addition to voltage changes due to phase currents [17]. Customer voltage rise is likely to be of concern in radial networks, which are commonly constructed with feeders covering long distances with relatively low current capacity conductors. In such networks, excessive voltage rise can even be initiated by small DER penetrations

TABLE I
SUGGESTED LIMITS FOR LOADING ABOVE NAMEPLATE RATING FOR DISTRIBUTION TRANSFORMERS [19]

Top-oil temperature	120 $^{\circ}C$
Hottest-spot conductor temperature	200 $^{\circ}C$
Short-time loading (1/2 h or less)	300%
Average loss of life per day in any emergency operation	4%

due to high impedance of the long conductors. Moreover, these feeders are often operated close to the statutory upper voltage limit to counter the large voltage drop over the distribution lines.

B. Voltage unbalance

Voltage unbalance in three-phase distribution systems is a condition in which the three-phase voltages differ in amplitude or are displaced from their normal 120° phase relationship or both [3]. In European LV distribution networks, small-scale embedded generators (SSEGs) with maximum capacity equal or less than 5 kVA are normally single-phase generation units and are installed disproportionately on a single-phase along with the fact that their growth is consumer-driven and not centrally planned. Additionally, the level of unbalance in LV distribution grids depends on phase-conductor configurations, such as unsymmetrical spacing between phase conductors [18].

The percentage voltage unbalance factor (VUF) is used to define the acceptable level of unbalance and is calculated by (3).

$$VUF(\%) = \frac{V_2}{V_1} \times 100\% \tag{3}$$

The negative V_2 and the positive V_1 sequence components of every node are computed by (4).

$$\begin{bmatrix} V_0 \\ V_1 \\ V_2 \end{bmatrix} = \frac{1}{3} \begin{bmatrix} 1 & 1 & 1 \\ 1 & a & a^2 \\ 1 & a^2 & a \end{bmatrix} \begin{bmatrix} V_a \\ V_b \\ V_c \end{bmatrix} \tag{4}$$

$$a = 1\angle 120^{\circ}$$

where:

V_0, V_1, V_2	zero, positive and negative sequence voltage components,V
V_a, V_b, V_c	phase-neutral voltages,V

Under normal operating conditions, the measured VUF at any node must remain below 2% during each period of one week for at least 95% of the week [16].

C. Thermal constraints

Transformer and distribution network lines have a thermal rating determined by the maximum current carrying capacity of that component. If a component is loaded above its thermal rating for an extended period of time, it will overheat, leading possibly to permanent damage, or even to a dangerous event, such as fire or explosion [3].

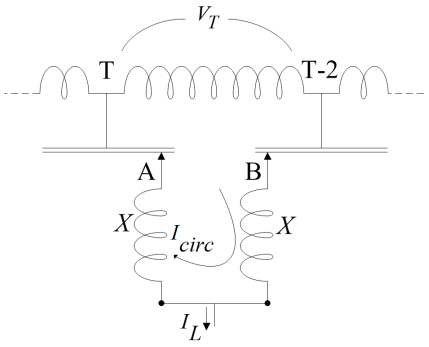

Fig. 2. Reactance type OLTC

1) Transformer thermal limits: Secondary transformers are referred to in terms of operating voltage and nominal kVA rating. Their kVA rating indicates the amount of apparent power that can be transferred between their two sets of terminals. At low demand and high SSEGs penetration scenarios, the power generation may exceed local demand. This would cause the surplus power to be fed into MV systems through distribution transformers, which in extreme cases might exceed nominal ratings. Until recently, distribution transformers were fitted with off-load tap changers, therefore this rating was symmetrical and did not vary with the power flow direction. However, reverse power flows may present a more significant problem for transformers fitted with OLTCs. The OLTC mechanism can impose an asymmetrical power flow limit, causing great rating reduction when power flows in the reverse direction [20].

Following the computation method of loading capability given in Standard C57.91-1995 [19], "IEEE Guide for Loading Mineral-Oil-Immersed Transformers," the maximum peak load that can be impressed on an oil-immersed transformer per timestep is calculated. First, the mean values of the winding hottest-spot temperature, the top-oil temperature and the equivalent aging of the transformer are computed daily step-by-step for all 10-minutes time intervals. Next, the equivalent aging factor and the loss of life percentage are calculated for each day of the year. A comparison is made between the calculated and the limiting values shown in Table I. Violations to any of these limitations lead to maximum loading capacity exceedance.

As for the OLTC, its type plays the main role in the limitation of loading capacity. According to [21], unlike single resistor type, reactor and double resistor type tap-changers do not limit the reverse power flow capacity. Making the assumption that the investigated transformer is fitted with reactor type OLTC, the inverse and reverse power flow capacities are considered to be equal for this work. As displayed in Fig. 2, the most onerous switching regime for the tap-changer is the transition from tap position T to T-2 due to the additional circulating current I_{circ} which is equal to V_T/X. C57.131, "IEEE Standard Requirements for Tap Changers", shows that in this regime, current $(1/2I_L + I_{circ})$ is switched under recovery voltage $(V_T + 1/2jXI_L)$, where I_L is the load current and X is the reactance of the preventive autotransformer [22]. Considering that the maximum loading capability is limited by constraints on permissible switched

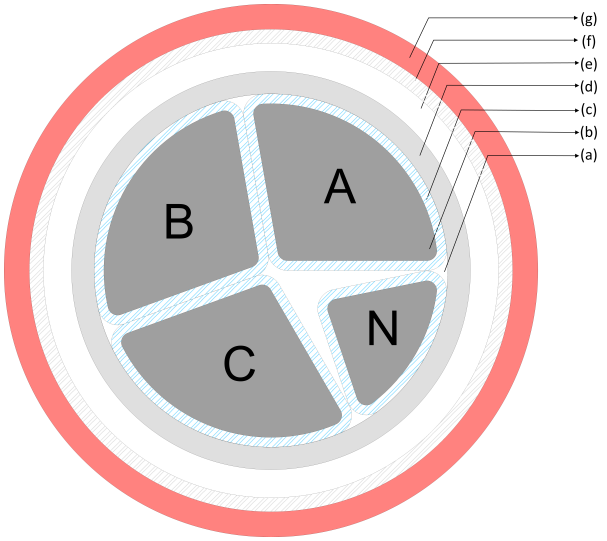

Fig. 3. Investigated sector-shaped conductor cable consists of the following layers: (a) filler of asphalted jute , (b) copper conductor, (c) paper insulation, (d) lead sheath, (e) asphalted jute, (f) steel tapes armouring and (g) PVC or asphalted jute

current I_{max}, recovery voltage V_{max} and switched kVA S_{max}, the load current I_L must fulfill the constraints (5)-(6) at every timestep:

$$\left|\frac{\overrightarrow{I_L}}{2} + \overrightarrow{I_{circ}}\right| \leq I_{max}, \quad \left|\frac{jX\overrightarrow{I_L}}{2} + \overrightarrow{V}_T\right| \leq V_{max} \tag{5}$$

$$\left|\frac{\overrightarrow{I_L}}{2} + \overrightarrow{I_{circ}}\right| \cdot \left|\frac{jX\overrightarrow{I_L}}{2} + \overrightarrow{V}_T\right| \leq S_{max} \tag{6}$$

When any of the above constraints is violated, the maximum loading capacity is exceeded.

2) Cable thermal limits: Knowledge of the cable thermal response is attained by the development of a thermal model which considers the heat generated in the cable, as well as the heat transfer capability of the cable and its surroundings. More specifically, this model consists of thermal capacitances and resistances formed by the constituent parts of the cable itself and its surroundings. In the literature, various thermal ladder networks have been reported, making the assumption of equally-loaded conductors [23]–[27]. Regarding that the phase loadings in real LV distribution lines are unbalanced, one individual thermal network can be considered for each conductor. However, this approach omits the thermal interaction between the conductors rendering its application difficult for LV cables. In addition, the investigated LV cable consists of sector-shaped conductors as shown in Fig. 3 and

TABLE II
VALUES OF PROPERTIES FOR THE CABLE MATERIALS

Material	Heat capacity [J]	Density $[kg/m^3]$	Thermal conductivity [W/(m*K)]
Copper	385	8700	400
Paper	0.833x10^{-3}	1200	0.1667
asphalted jute	1.8181x10^{-3}	1100	0.1667
lead	130	11300	35
steel	466	7850	17
soil	800	1800	0.2857

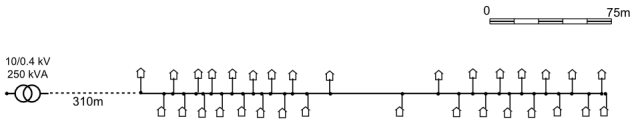

Fig. 4. Investigated LV grid

the neutral conductor N has different cross-section from the phase conductors (A, B and C). Although in [28], Simons has proposed an empirical formula for the calculation of the thermal resistance between sector-shaped conductors and sheath, its main requirement is the same cross-section for all the conductors. Such approximations and assumptions lead to inaccuracies in the calculations and often force cable engineers to use unnecessarily large safety factors and overly conservative designs. In this paper, a finite-element method is applied via the 2-D finite element software COMSOL Multiphysics for the calculation of the temperature distribution over the cable. The system consists of the displayed cable located in the centre of a square representing the soil. When the temperature distribution over the cable is calculated, the mean 10-minutes temperatures on the paper insulation of the conductors are compared with the maximum permitted insulation temperature. Any violation of this limitation result in exceeding the maximum loading capacity of the cable. More details about the geometry and the cable are given in the next section.

IV. SIMULATIONS

At first, the necessary inputs and assumptions of the investigated grid are described, followed by the introduction of the simulation outputs. The simulation results and conclusions are analyzed at the end of the section.

A. Inputs and assumptions

A real Flemish LV urban grid was provided by the Belgian utilities and serves as a basis for the following simulations. As displayed in Fig. 4, the investigated LV grid comprises 39 households, whereof 10 are considered single-phase.

Each phase is linked to an individual annual load profile with a step size of 10 min. The load profiles given by the same utilities only provide active power consumption per time step, hence, a random power factor distribution of [0.85-1] was assumed [29]. Furthermore, profiles that exceed the maximum permitted current per single-phase consumer, 63 A, are rejected. The remaining profiles are randomly distributed among the households. As of April 2013, in Flanders more than 99% of the approved applications for DERs installations are related to PVs [30]. Since in this

TABLE III
THICKNESS OF THE CABLE LAYERS

Material	Thickness [mm]
Paper insulation	0.7
Lead sheath	1.6
asphalted jute	2
steel armouring	1
outer serving	2

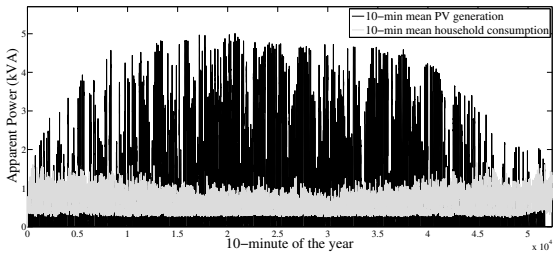

Fig. 5. 10-minutes mean PV generation and household consumption

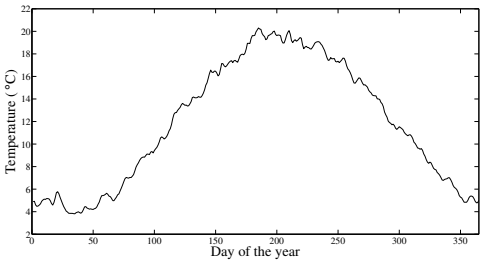

Fig. 6. Soil temperature over the period of one-year

study, voltage unbalance issues are also investigated, only single-phase PVs of 5 kVA are considered. Their rating was selected according to the maximum permissible installed peak power for single-phase SSEGs. In addition, these units are connected to the same phase with the single-phase loads and to random phase with the three-phase loads. Considering the prohibition of reactive power delivery at LV grids, the power factor of PVs is set to 1. This approach represents a worst-case scenario for the network operation, therefore, the diversity of PV systems is omitted (e.g shadowing phenomena, various module tilt angles and orientation). The measured solar radiation data were provided by HelioClim over a period of one year (2005) in 15-min step sizes and interpolated to 10-min average values. A 120-W reference module was selected for the dc power generation assuming a total efficiency of 85% for the additional equipment (inverter, cables). Finally, the normalized ac power output was reformed in order to represent a 5 kW PV unit. Fig. 5 displays the 10-minutes mean PV generation as well as the average 10-minutes consumption of the used load profiles.

The distribution cables of this grid are underground and the depth of burial is assumed to be 0.7 m under the soil surface. Moreover, the effect of other nearby cables, gas or water pipes is omitted. As for the cable that connects the distribution cable with the household meter, its rating is calculated taking into account the total installed household capacity. When the consumer wants to increase this capacity, the DSO inquires the need for its replacement. Consequently, it is more crucial to investigate the thermal behaviour of the distribution cable. As mentioned in the previous section, the distribution cable is four-core, sector-shaped conductor with cross-section 3x70 + 1x50 mm^2 and maximum paper insulation temperature equal to $80°C$. Table II and III illustrate the values of properties for the cable materials and the thickness of each layer respectively. The measured soil temperature data were provided by the Belgian Meteorological Institute (KMI) over a period of eight years in one-day mean values at 0.5 m depth for a place near to the investigated network. Regarding issues of data representativeness, the one-day mean measurements were averaged over the whole period and used as reference temperature via the superposition of the results. A crucial observation that Vidal concluded in [32], and is shown in Fig. 6 as well, is the sinusoidal variation of the soil temperature over the year.

Finally, the oil-type distribution transformer of 250 kVA capacity is fitted with a reactor type OLTC, regulating the upper voltage. Technical characteristics of the evaluated device are given in Table IV.

According to [33], the load forecasts for the year 2020 indicate that in Flanders the actual load base can either increase up to 103.78% or decrease till 96%. The set of scenarios includes both possible changes, as well as the actual load base 100%. As for the PV units, they are randomly located among the grid considering their penetration level. In this paper, the penetration level of DER's is expressed as the percentage of the transformer capacity. Table V displays the investigated scenarios of different PV penetration levels. This set of scenarios is combined with the three load bases (96%, 100% and 103.78%) resulting in 12 different cases taking into account the initial scenario with 0% penetration level.

B. Simulation outputs

For each scenario, the annual load flow is simulated via the power systems analysis software DIgSILENT PowerFactory and the OLTC incorporation is evaluated via a set of variables. Considering the technical impacts described in section III the study provides 4 main outputs related to power quality:

1) Over-voltage indicator: 100th voltage percentile (maximum voltage, during 100% of the time), which is compared with the over-voltage limit (110% U_n).
2) Under-voltage indicator (1): 5th voltage percentile representing the distance to the first under-voltage limit (90% U_n).
3) Under-voltage indicator (2): 0th voltage percentile

TABLE IV
TECHNICAL CHARACTERISTICS OF THE EVALUATED OLTC [31]

Maximum number of operating positions	17
Step voltage per tap-change	1.8%
Maximum rated step voltage	600 V
Maximum rated through current	30 A
Maximum step capacity	9 kVA
Inductance of the preventive autotransformer (approximate value)	269 mH

TABLE V
SPECIFICATION OF THE INVESTIGATED SCENARIOS

Penetration level	Additional PV capacity	Additional PVs
+20%	50 kWp	10
+30%	75 kWp	15
+40%	100 kWp	20
+50%	125 kWp	25

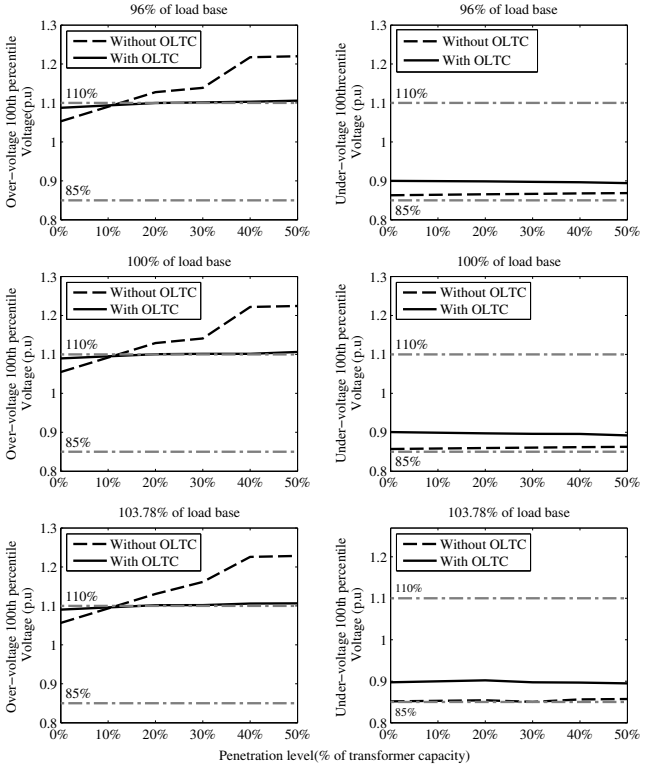

Fig. 7. 100th voltage percentiles

(minimum voltage, during 100% of the time), which is compared with the lowest voltage limit (85% U_n).

4) VUF 95th percentile, which represents the distance to the standard limit (2 %) during 95% of the time.

Apart from the above power quality outputs, the total annual energy losses are calculated for each scenario. In addition, the over-voltage indicator and under-voltage indicator (2) of the simulations without the OLTC determine the maximum number of operating positions for the OLTC. Concerning the evaluation of the thermal models, five different outputs are investigated during 100% of the time:

1) Top-oil temperature indicator: maximum 10-min top-oil temperature, which can be considered as the distance to the top-oil temperature limit of the transformer ($120°C$).
2) Hottest-spot conductor temperature indicator: maximum 10-min hottest-spot conductor temperature, representing the distance to the highest transformer limit ($200°C$).
3) Short-time loading indicator: maximum 10-min loading, which is compared with the maximum permitted loading of the transformer (300%).
4) Loss of life indicator: maximum average daily loss of transformer life, which can be considered as the distance to the maximum value of 4%.
5) Paper insulation temperature indicator: maximum 10-min temperature of paper insulation, which is compared with the highest value of the cable ($80°C$).

Finally, the violations of the OLTC constraints are considered based on the following three outputs during 100% of the time:

1) Switched current through tap-changer: 10-min current through the tap-changer, which is compared with the maximum limit (30 A).
2) Recovery voltage on the tap-changer: 10-min recovery voltage of the tap-changer, which is compared with the highest value (600 V).
3) Apparent power of the tap-changer: 10-min apparent power of the tap changer, which is compared with the maximum permitted power (9 kVA).

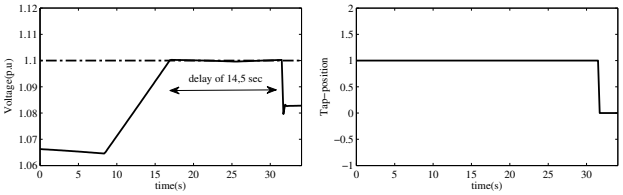

Fig. 8. Dynamic response of the OLTC: (a) Phase-to-neutral voltage of the node with over-voltage (b) Tap-changer response

C. Simulation results

The results obtained from the simulations are of interest so as to understand the OLTC operation, and clarify its advantages and drawbacks for the LV distribution networks.

As shown in Fig. 7, for all the scenarios with 0% PVs penetration level, the OLTC causes rise of the over-voltage indicators because the tap-position increases in order to compensate the load voltage drop. Moreover, the over-voltage indicator does not exceed the statutory limit (110% U_n) by reason of the absense of generation. While connecting PVs in the grid, the violations of the over-voltage indicator activate the tap-position drop. Though the tap-changer decreases the over-voltage indicator, it cannot stay below 110% in most cases. Some reasons why this trend occurs are the finite response time of both the tap-changer and the comparators as well as the voltage measurement time from the remote units. Fig. 8 displays one specific time interval when the tap-position rise is activated due to an over-voltage violation with a delay of 14,5 sec. As for the simultaneous under-voltage and over-voltage violations, they never occur for the investigated scenarios, so the tap-changer is activated when it is mandatory.

Concerning the under-voltage indicators, Fig. 7 and Fig. 9 illustrate the 100th and 95th under-voltage percentiles, respectively. Even though they never exceed the statutory limits, the tap-changer improves their values. As it can be observed in the same figures, the improvement of indicator (2) is more perceptible than of indicator (1). Besides, the contribution of the OLTC is determinant for scenarios with 103.78% load base, since the 100th under-voltage percentile approximates its limit value (0.85 p.u).

The compliance with the power quality regulations also depends on the voltage unbalances. From the simulation results, it was concluded that the independent OLTC control of every phase leads to voltage unbalance problems. For the scenarios without PVs, the unbalances originate from the random distribution of both the single-phase loads among the phases and the various power profiles among the loads.

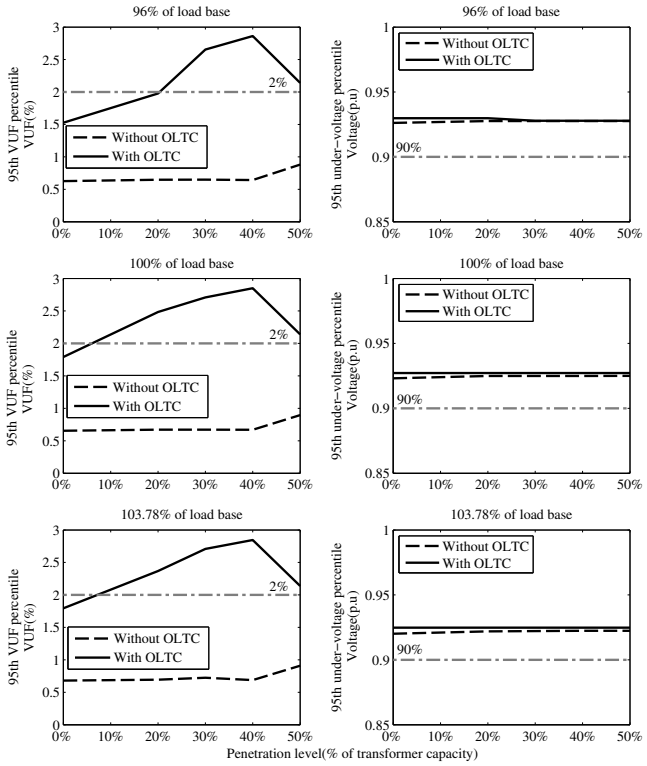

Fig. 9. 95th voltage percentiles

Moreover, even though the uncoordinated connection of additional PVs increases the 95th VUF percentile, the standard limit is not exceeded without the OLTC application (Fig. 9). On the contrary, when the OLTC is fitted to the transformer, the 95th VUF percentile in most cases exceeds the maximum permitted value (2%). As it was observed, the OLTC can increase the negative sequence of the supply voltage, because the controller considers only the magnitude of the phase-to-neutral voltages.

The annual network losses are also affected by the OLTC integration. From Fig. 10, it is noticeable that the OLTC reduces network losses and this trend becomes more perceptible as the load base increases. This can be an additional motivation for DSO's to fit this device to the distribution transformers in the future. However, the rise of the network losses for the scenarios of 50% penetration level shows that the OLTC can deteriorate this parameter under high DG integration conditions.

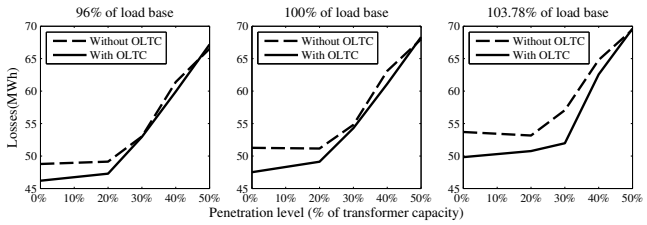

Fig. 10. Annual network losses

As for the thermal constraints of both the transformer and the cable, no violations of the maximum top-oil, hottest-spot conductor and paper insulation temperatures were noted. In addition, as shown in Fig. 11, for the scenarios of 0%, 20% and 30%, the maximum differences of the same outputs ($\Delta\theta = \theta_{without-OLTC} - \theta_{with-OLTC}$) are negligible, when fitting the tap-changer. While for the scenarios of 40% the temperatures display a more distinct drop, they follow different trend for the scenarios of 50%. More specifically, the top-oil and hottest-spot temperatures decrease slightly, unlike with the paper insulation temperature which increases integrating the OLTC. Considering the network losses rise for that scenario, the paper insulation temperature is expected to increase.

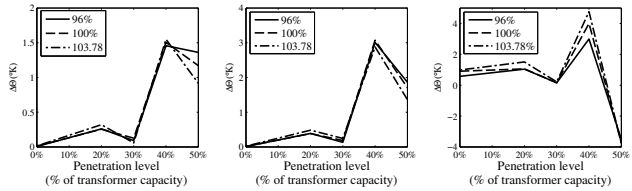

Fig. 11. Maximum temperature differences for the investigated load base levels fitting the OLTC: (a) Top-oil temperature (b) Hottest-spot conductor temperature (c) Paper insulation temperature

Concerning the maximum short-time loading and average loss of life for the transformer, no violations were indicated. As it can be understood from Fig. 12, the maximum short-time loading follows the same trend with the temperature indicators of the transformer. Regarding the maximum average loss of life, it is almost constant at 0.78% for all the cases regardless from the presence of the tap-changer.

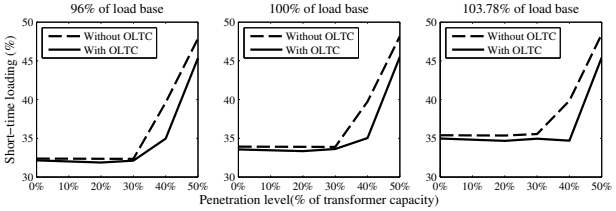

Fig. 12. Maximum short-time loading of the transformer

Finally, from the evaluation of the outputs related to the OLTC constraints, no violations were found (Fig. 13). Even though the evaluated parameters increase while connecting more PVs, they never exceed the mentioned limits.

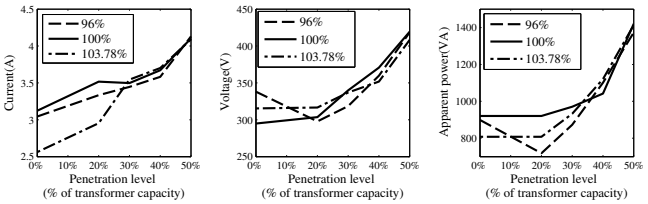

Fig. 13. OLTC parameters for the investigated load base levels: (a) Maximum switched current through the tap-changer (b) Maximum recovery voltage (c) Maximum step capacity

V. Conclusions

This paper assesses a proposed voltage control method for the OLTC via a set of technical parameters related to the power quality and the thermal models of the grid components. It is shown that this technique can partly improve

the over-voltage and the under-voltage indicators due to the discrete time response of the appliances. Furthermore, the individual OLTC control of every phase deteriorates the voltage unbalances in the grid. As for the annual network losses and the paper insulation temperature of the cables, the OLTC integration decreases them slightly, however, they can increase under high DER penetration levels. On the other hand, the temperature indicators of the transformer display a distinct drop only under the above conditions. While the maximum short-time loading follows the same trend with the temperature indicators, the maximum average loss of life seems to be unaffected by the presence of the tap-changer. In future work, the proposed voltage control algorithm will be combined with the operation of additional ANM technologies which aim to solve the above identified issues.

ACKNOWLEDGMENT

The work is supported via the project Active Substations organised by EIT Knowledge & Innovation Commmunity (KIC) InnoEnergy. The authors would like to thank the Belgian Meteorological Institute (KMI), HelioClim and the Belgian utilities for providing the necessary data for the simulations. T. Wijnhoven has a Ph. D. fellowship of the Research Foundation - Flanders (FWO) and wishes to acknowledge the financial support of the FWO.

REFERENCES

[1] P. Trichakis, P. C. Taylor, P. F. Lyons, and R. Hair, "Predicting the technical impacts of high levels of small-scale embedded generators on low-voltage networks," *IET Renew. Power Gener.*, vol. 2, no. 4, pp. 249–262, 2008.

[2] A. Soroudi, M. Ehsan, R. Caire, and N. Hadjsaid, "Possibilistic Evaluation of Distributed Generations Impacts on Distribution Networks," *IEEE Trans. Power Syst.*, vol. 26, no. 4, pp. 2293–2301, 2011.

[3] R. C. Dugan, M. F. McGranaghan, S. Santosa, and H. W. Beaty, *Electric Power Systems Quality*, 2nd ed. McGraw-Hill, 2002.

[4] C. Masters, "Voltage rise: The big issue when connecting embedded generation to long 11 kV overhead lines," *Power Eng. J.*, vol. 16, no. 1, pp. 5–12, 2002.

[5] "Deutsche Energie-Agentur GmbH (dena), dena-Verteilnetzstudie: Ausbau- und Innovationsbedarf der Strom- verteilnetze in Deutschland bis 2030., Berlin, 2012," Tech. Rep., 2012.

[6] T. Xu and P. C. Taylor, "Voltage Control Techniques for Electrical Distribution Networks Including Distributed Generation," in *IFAC*, no. 1, 2008, pp. 11 967–11 971.

[7] B. O. Brewin, S. C. E. Jupe, M. G. Bartlett, K. T. Jackson, and C. Hanmer, "New technologies for low voltage distribution networks," in *Innovative Smart Grid Technologies (ISGT)*, Dec. 2011, pp. 1–8.

[8] M. J. Heathcote, *The J & P Transformer Book*, 12nd ed. Cend,FIEE.

[9] C. Gao and M. A. Redfern, "A Review of Voltage Control Techniques of Networks with Distributed Generations using On-Load Tap Changer Transformers," in *Universities Power Engineering Conference UPEC*, 2010, pp. 3–8.

[10] P. Kadurek, J. F. G. Cobben, and W. L. Kling, "Smart MV/LV transformer for future grids," in *Power Electronics Electrical Drives Automation and Motion (SPEEDAM), International Symposium*. IEEE, Jun. 2010, pp. 1700–1705.

[11] C. Reese, C. Buchhagen, and L. Hofmann, "Voltage range as control input for OLTC-equipped distribution transformers," in *Transmission and Distribution Conference and Exposition (T&D), IEEE PES*. IEEE, May 2012, pp. 1–6.

[12] W. Yan, M. Braun, J. V. Appen, E. Kämpf, M. Kraiczy, C. Ma, T. Stetz, and S. Schmidt, "Operation Strategies in Distribution Systems with High Level PV Penetration," in *Solar World Conference*, 2012, pp. 1–8.

[13] D. Dohnal, "On-Load Tap-Changers for Power Transformers-A Technical Digest," Regensburg: MR Publication, Tech. Rep.

[14] J. Faiz and B. Siahkolah, *Electronic tap-changer for distribution transformers*, 1st ed. Springer, 2011.

[15] "Synergrid, C10/11:Specifieke technische voorschriften voor decentrale productie-installaties die in parallel werken met het distributienet (in Dutch)," Synegrid, Tech. Rep., 2012.

[16] "Nen-EN 50160 Voltage characteristics of electricity supplied by public electricity networks," Tech. Rep., 2010.

[17] L. Degroote, B. Renders, B. Meersman, and L. Vandevelde, "Neutral-point shifting and voltage unbalance due to single-phase DG units in low voltage distribution networks," in *2009 IEEE Bucharest PowerTech*. Ieee, Jun. 2009, pp. 1–8.

[18] A. V. Jouanne and B. B. Banerjee, "Assessment of Voltage Unbalance," *IEEE Transactions on Power Delivery*, vol. 16, no. 4, pp. 782–790, 2001.

[19] T. Committee, "IEEE Guide for Loading Mineral-Oil- Immersed Transformers," IEEE Standard C57.91, Tech. Rep., 2003.

[20] L. M. Cipcigan and P. C. Taylor, "Investigation of the reverse power flow requirements of high penetrations of small-scale embedded generation," *IET Renewable Power Generation*, vol. 1, no. 3, pp. 160–166, 2007.

[21] V. Levi, M. Kay, and I. Povey, "Reverse power flow capability of tap-changers," in *Proc. Int. Conf. on Electricity Distribution (CIRED)*, vol. 2, no. June, 2005, pp. 6–9.

[22] I. Power and E. Society, "IEEE Standard Requirements for Tap Changers," IEEE Std C57.131, Tech. Rep. May, 2012.

[23] J. H. Neher, "The Transient Temperature Rise of Buried Cable Systems," *IEEE Transactions on Power Apparatus and Systems*, vol. 83, no. 2, pp. 102–114, Feb. 1964.

[24] F. Buller, "Thermal transients on buried cables," *Transactions of the American Institute of Electrical Engineers,*, vol. 70, no. 1, pp. 45–55, 1951.

[25] F. C. Van Wormer, "An Improved Approximate Technique for Calculating Cable Temperature Transients," *Power Apparatus and Systems, Part III. Transactions of the American Institute of Electrical Engineers*, vol. 74, no. 3, pp. 277–281, 1955.

[26] CIGRE, "Current ratings of cables for cyclic and emergency loads. Part 1. Cyclic ratings (load factor less than 100%) and response to a step function," *Electa*, no. 24, pp. 63–69, 1972.

[27] "IEC Std. 60853-1, Calculation of the cyclic and emergency current ratings of cables. Part 1: Cyclic rating factor for cables up to and including 18/30 (36) kV," Tech. Rep., 1985.

[28] D. M. Simons, "Cable Geometry and the Calculation of Current-Carrying Capacity," *Transactions of the American Institute of Electrical Engineers,*, vol. XLII, no. 2, pp. 600–620, Jan. 1923.

[29] W. Labeeuw and G. Deconinck, "Customer Sampling in a Smart Grid Pilot," in *IEEE PES GM'12*, 2012, pp. 1–7.

[30] "VREG Statistics, Productie-installaties in Vlaanderen waarvoor groenestroomcertificaten worden toegekend (in Dutch)," Tech. Rep., 2013.

[31] MR, "GRIDCON iTAP, The system solution for voltage regulated distribution transformers," Tech. Rep., 2012.

[32] J. Vidal, "Determination des pertes calorifiques dans les canalisations enterres," Ph.D. dissertation, Editions SIC, Brussels, 1961.

[33] "Energie- en broeikasgasscenarios voor het vlaams gewest," Vlaamse Instituut voor Technologisch Onderzoek (VITO), Tech. Rep.